Membrane-Forming Properties of Cationic Lipids Bearing Oxyethylene-Based Linkages

Santanu Bhattacharya* and Padinjarae Vangasseri Dileep

Department of Organic Chemistry, Indian Institute of Science, Bangalore 560 012, India

Received: October 22, 2002; In Final Form: January 1, 2003

The membrane-forming properties of four cationic lipids (**1**−**4**) having varying number of oxyethylene $(-CH_2-CH_2-O-)_n$ units at the linkage region between the pseudo-glyceryl backbone and the hydrocarbon chains have been described. Lipids **1** and **2** have an equal number of oxyethylene units attached to both C-1 and C-2 positions of the pseudo-glyceryl backbone, while the other two, **3** and **4**, are unsymmetrical in terms of the number of oxyethylene linkages. The membrane characteristics of these lipids were compared with a control lipid, **5**, bearing just an ether functionality at both the C-1 and C-2 positions. All the lipids (**1**−**5**) formed stable suspensions in water which showed the presence of membranous aggregates as revealed by electron microscopy (TEM). The lipids **1**, **2**, and **4** showed distinct spherical aggregates in TEM, whereas **3** exhibited particles of irregular morphologies. The lipid suspensions were further characterized by dynamic light scattering and zeta potential measurements. Except for lipid **3**, zeta potentials of such lipid aggregates were found to be substantially lower than their diether analogue, **5**. X-ray diffraction studies with the lipid cast films revealed that incorporation of oxyethylene units at the linkages increased the unit bilayer thickness of the membranous assemblies. Temperature-dependent fluorescence anisotropy experiments using the lipid-soluble probe 1,6-diphenylhexatriene (DPH) suggested a disordered environment in these lipid aggregates even in their gel states. The aggregates formed by lipid **3** showed the lowest DPH anisotropy values. Clear thermotropic phase transitions typical of membranous assemblies were observed for all the lipid suspensions by differential scanning calorimetry. The phase transitions were reversible and exhibited large hysteresis indicating that the observed phase transitions were of first order.

1. Introduction

The design, synthesis, and characterization of cationic lipid formulations are attracting much attention nowadays, mainly due to their application as nonviral gene delivery vectors.[1−7] The linkage region between the pseudo-glyceryl backbone and the hydrocarbon chain is a critical segment of the lipid bilayer. In the aqueous suspension of a lipid, the center of the lipid bilayer as well as the part comprising its hydrocarbon chains has a low dielectric constant environment compared to the bulk water. This leads to a drastic transition in polarity at the interfaces, i.e., at the location of the linkage, the glyceryl backbone, and the headgroup.[8] Due to this, even small changes in the linkage functionalities between the hydrocarbon chain and the pseudo-glyceryl backbone bearing the polar headgroup of a lipid molecule exert a marked influence on its aggregation properties when it is suspended in water.[9,10] Such subtle modulations at the linkage regions of a cationic lipid have been shown to influence their transfection efficiencies significantly. For instance, *N*-(1-[2,3-dioleyloxy]propyl)-*N*,*N*,*N*-trimethylammonium chloride (DOTMA), which contains *ether* links between the headgroup and the long alkyl chain, is shown to have much greater in vivo transfection efficiency than the corresponding cationic lipid with *ester* linkage, *N*-(1-[2,3-dioleoyloxy]propyl)-*N*,*N*,*N*-trimethylammonium chloride (DOTAP).[4,11] The importance of linkage functionalities in modulating the gene transfection efficiencies of cationic cholesterol amphiphiles has also been demonstrated.[12,13]

* Corresponding author. E-mail: sb@orgchem.iisc.ernet.in. Also at Chemical Biology Unit, JNCASR, Bangalore, 560 012, India.

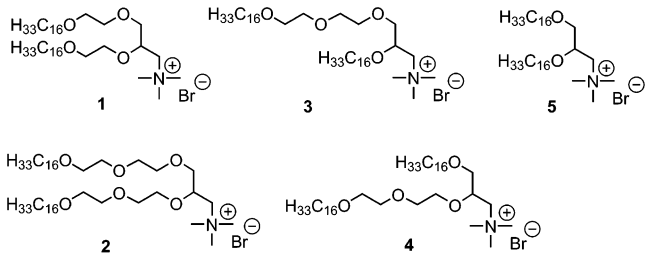

Figure 1. Molecular structures of the cationic lipids mentioned in the present study.

Recently we reported the synthesis of four lipids **1**−**4** (Figure 1) having hydrophilic oxyethylene units at the linkage region.[14] Among these, the lipids **1** and **2** bear $(-CH_2-CH_2-O-)_n$ units at both C-1 and C-2 positions of the pseudo-glyceryl backbone, making their linkage regions identical, whereas **3** and **4** carry only one $(-CH_2-CH_2-O-)_2$ unit either at the C-1 or C-2 position of the backbone, rendering the resulting systems unsymmetrical. Hydrophilic polyoxyethlyene units at the headgroup regions of lipid molecules are known to have important biological and pharmaceutical effects.[15,16] However, the influence of such $(-CH_2-CH_2-O-)_n$ groups at the linkage region of a lipid on its aggregation properties have not yet been addressed. Incorporation of $(-CH_2-CH_2-O-)_n$ groups at the linkage regions were expected to increase the interfacial hydration in such aggregates. Such variations at the interfacial region should in turn influence the association of these assemblies with various biomolecules such as double-stranded DNA.

10.1021/jp0272771 CCC: $25.00
Published on Web 04/02/2003

We observed that incorporation of oxyethylene units significantly enhances the in vitro transfection efficiencies of glycerol based cationic lipids.[17] Interestingly, the transfection efficiencies of these lipids were found to be refractory to the presence of serum proteins, which is rather unusual.[18] Thus, though unnatural, these synthetic lipid molecules represent an important class that deserves detailed examination. In this context, we sought to examine the aggregation behavior of such lipid molecules. Herein we describe the detailed membrane-forming characteristics of these biologically important lipid molecules. To put things in proper perspective, we have compared the membrane-forming properties of this series of molecules with that of a known cationic lipid, **5**, having just ether links.

2. Experimental Section

2.1. General. All the reagents, molecular probes, and chemicals used in this study were of the highest purity available. Cationic lipids **1**−**5** were synthesized as reported[14] and were characterized fully by their IR spectra, ^{1}H NMR spectra, mass spectra, and elemental analysis. The purity of the lipids was checked by thin-layer chromatography (TLC) on silica gel G-60 plates (Merck) prior to vesicle preparation.

2.2. Vesicle Preparation. Thin lipid films from individual lipids **1**−**5** were prepared in Wheaton glass vials by dissolving weighed amounts of individual lipids in chloroform and evaporating the organic solvent under a steady stream of dry nitrogen. The last traces of organic solvent were removed by keeping these films under high vacuum overnight. Water was added to each individual film and was kept for hydration at 4 °C for 6−10 h. Then these samples were repeatedly freeze−thawed (ice-cold water to 50 °C) with intermittent vortexing. Multiwalled vesicle-like aggregates (MLVs) were present in these suspensions as revealed from electron microscopy (see below). Small single-walled aggregates were prepared by sonicating these MLVs in a bath sonicator above the phase transition temperature of the individual lipids for 10−15 min.

2.3. Transmission Electron Microscopy (TEM). Lipid suspensions (1 mM) were examined under transmission electron microscopy by negative staining with 1% uranyl acetate. Sonicated suspensions were spread onto carbon−Formvar coated copper grids (400 mesh), and the vesicles were allowed to settle onto the grid. Excess solution was wicked off using a filter paper, and the grid was air-dried for 30 min before examination under TEM. TEM was performed on a JEOL 200-CX electron microscope, typically with an accelerating voltage of 100 keV. Micrographs were recorded at a magnification of 80 000.

2.4. Dynamic Light Scattering (DLS). The 0.33 mM unilamellar vesicular suspensions prepared in pure water (Millipore) were used for light scattering measurements. Experiments were performed using a Malvern Zetasizer 3000 instrument, which employed an incident laser beam of 633 nm. An interfaced autocorrelator was used to generate the full autocorrelation of the scattered intensity. The time-correlated function was analyzed by the method of cumulants, and the calculations yielded specific distribution of particle size populations. The values reported are the average of two independent experiments, each of them having 10 subruns. The instrument was calibrated using standard polystyrene nanospheres (Duke Sci. Corp., Palo Alto, CA) of 96 ± 3 nm size distribution.

2.5. Zeta Potential Measurements. Unilamellar vesicles (1 mM) prepared as mentioned in section 2.2 were diluted to 0.06 mM and used for zeta potential measurements using a Malvern Zetasizer 3000 electrophoretic light scattering instrument. The values are reported as an average of 10 cumulative runs along with standard deviations.

2.6. Cast-Film X-ray Diffraction Measurements. The experiment was done following the reported procedures.[19,20] A multilamellar suspension of each lipid (3 mM) in water was placed on a precleaned glass plate which, upon air-drying, afforded a thin film of the lipid aggregate on the glass plate. X-ray diffraction of an individual cast film was performed using the reflection method with a Rich Seifert-3000 TT X-ray diffractometer. The X-ray beam was generated with a Cu anode, and the Cu Kα beam of wavelength 1.54 Å was used for the experiments. Scans were performed for θ values up to 10°.

2.7. Fluorescence Anisotropy Measurements. For the preparation of lipid suspensions doped with fluorescent probe, 1,6-diphenylhexatriene (DPH), the probe in dry THF was cosolubilized with a given lipid in chloroform. A thin film was generated upon evaporation of solvent in the dark, and then DPH-doped unilamellar vesicles (lipid concentration = 1.5 mM) were prepared by freeze−thaw method as mentioned above. The final concentration of DPH in the vesicles was 0.01 mol % with respect to the lipid.

Steady state fluorescence anisotropies sensed by DPH doped in the vesicles were measured in a Hitachi F-4500 spectrofluorimeter equipped with polarizers upon excitation of DPH at 360 nm. The emission intensity was followed at 428 nm. The slit widths were kept at 5 nm for both the excitation and the emission. The fluorescence intensities of the emitted light polarized parallel (I_{VV}) and perpendicular to the excited light (I_{VH}) were measured at different temperatures. These fluorescence intensities were corrected for scattered light intensity. The fluorescence anisotropy values (r) at each temperature were calculated employing the equation $r = (I_{VV} - GI_{VH})/(I_{VV} + 2GI_{VH})$, where G is the instrumental grating factor.[21,22] The grating factor, G, was calculated using the equation $G = (I_{HV}/I_{HH})$, where I_{HV} and I_{HH} represent the fluorescence intensities of vertically polarized and horizontally polarized light, respectively, when a horizontally polarized light was used for the probe excitation. The gel to liquid crystalline phase transition temperatures (T_m) of each lipid were calculated from the midpoints of the breaks related to the temperature-dependent anisotropy values.[22−24] The temperature range for the phase transition was calculated from the two temperature points for each experiment that marked the beginning and the end of the phase transition process.

2.8. Differential Scanning Calorimetry (DSC). Multilamellar vesicles (1 mM) were prepared in degassed water as mentioned above, and their thermotropic behavior was investigated by high sensitivity differential scanning calorimetry using a CSC-4100 multicell differential scanning calorimeter (Calorimetric Sciences Corporation, Utah, USA). A baseline thermogram was obtained using degassed water in all the ampules including the reference cell to normalize cell to cell differences. For the baseline thermogram 0.5 mL of water was used. Samples were taken in the cells such that the differences in weight with the baseline experiment to the sample run was less than 0.001 g in the respective ampules. The measurements were carried out in the temperature range of 25−65 °C at a scan rate of either 10 or 20 °C/h. At least two consecutive heating and cooling scans were performed to confirm the reversibility of the transitions. The thermograms for the vesicular suspensions were obtained by subtracting the respective baseline thermogram from the sample thermogram using the software CpCalc provided by the manufacturer. The peak position in the plot of "excess heat capacity" vs temperature was taken as the solidlike gel to liquid crystalline phase transition temperature for each lipid suspension. The molar heat capacities, calorimetric enthalpies (ΔH_c), and

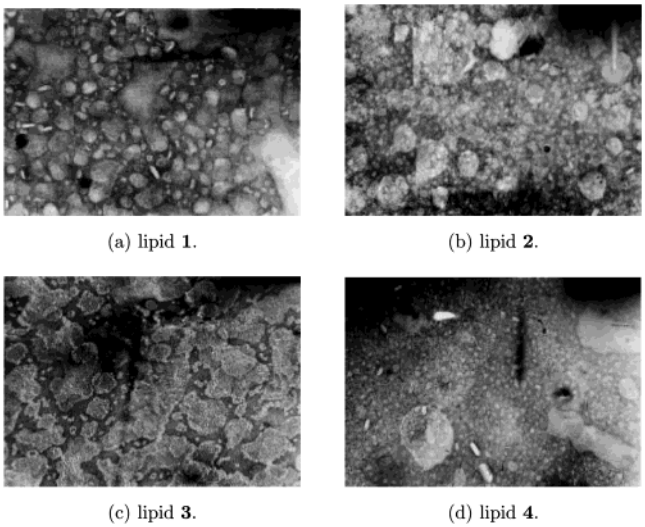

(a) lipid **1**. (b) lipid **2**. (c) lipid **3**. (d) lipid **4**.

Figure 2. Negative-stain transmission electron micrographs of aqueous suspensions of lipids **1**−**4** (scale 1 cm = 90 nm).

entropies (ΔS) were also computed using the same software. The size of the cooperativity unit has been calculated as

$$\mathrm{CU} = \frac{\Delta H_{\mathrm{vH}}}{\Delta H_{\mathrm{c}}}$$

where ΔH_{vH} is the van't Hoff enthalpy and ΔH_{c} is the calorimetric enthaply.[25] ΔH_{vH} has been calculated using the equation

$$\Delta H_{\mathrm{vH}} = \frac{6.9 T_{\mathrm{m}}^{\ 2}}{\Delta T_{1/2}}$$

where $\Delta T_{1/2}$ is the full width at half-maximum of the calorimetric thermogram and T_{m} is the phase transition temperature.[26]

3. Results

Upon hydration, the lipids having oxyethylene units at the linkage regions (**1**−**4**) were found to get dispersed in water with greater ease when compared to the lipid **5**, which was based on ether links alone. The suspensions formed from the lipids **1**−**4** were optically clear while that of **5** was found to be translucent. All the lipid molecules mentioned herein formed stable suspensions in water. No precipitation or noticeable increase in turbidity was observed even after 1 month when these suspensions were stored at 4 °C.

3.1. Aggregate Characterizations. Transmission electron microscope (TEM) images obtained for these lipid suspensions are shown in Figure 2. Generally, TEM examination of air-dried aqueous suspensions revealed the existence of closed aggregate structures for all four lipids **1**−**4**. The suspensions formed from lipids **1** and **2** having symmetrical chains showed as distinct aggregates in the micrographs (Figure 2a,b). The aggregates formed were mostly spherical in the case of the lipids **1** and **2** and had diameters in the range of 40−100 nm (Table 1). In contrast, lipid **3**, which has a dioxyethylene linkage only at the C-1 chain, formed closed aggregates of irregular morphologies as can be seen in Figure 2c. The average size range observed was 90−150 nm. Lipid **4** also formed closed aggregates (Figure 2d) which were larger (∼220 nm) in comparison with those observed with the other lipids.

The average hydrodynamic diameters of the individual lipid aggregates as revealed by dynamic light scattering (DLS) studies are presented in Table 1. All the lipid suspensions except **3** showed unimodal distributions of the aggregate populations. Aqueous suspensions of lipid **3** initially showed the existence of bimodal distributions which on aging averaged out to a broad distribution as evidenced from subsequent runs. It was observed that, in the case of symmetrical lipids, suspensions became increasingly monodisperse with the introduction of more and more oxyethylene groups at the linkage region. Under the above-mentioned conditions of vesicle preparation (section 2.2), lipid **2** yielded completely monodisperse suspensions. Polydispersity was higher for aggregates formed by lipid **3** as well as for lipid **5**. It may be noted that, in general, the aggregate sizes of lipid suspensions based on TEM studies were smaller than the hydrodynamic diameters obtained from the DLS studies. However, changes in the particle diameters follow the same trend in both TEM and DLS experiments. It is possible that the drying step in the TEM experiment might induce shrinkage of the aggregates to some extent.

TABLE 1: Average Diameter, Zeta Potential (ζ), and Aggregate Layer Width of the Lipid Suspensions of 1−5 in Water

lipid	size[a] (nm)	size[b] (nm)	ζ potential[c] (mV)	width[d] (Å)
1	150	40−80	19.2	54.5
2	160	55−100	25.2	59.2
3	140	90−150	45.0	53.8
4	240	220	20.7	52.1
5	260		40.1	48.7

[a] Hydrodynamic diameters obtained from DLS measurements. [b] As evidenced from TEM. [c] Standard deviation for these values were within ±3%. [d] Unit bilayer thickness from XRD experiments.

Next we measured the zeta potential of cationic lipid aggregates by laser Doppler spectroscopy. In this experiment, particle mobility in response to an electric field is measured by Doppler shifts of laser light.[27] The electrophoretic mobility of the particle in the electric field is then correlated to the zeta potential. This technique has been successfully applied for the characterization of surface groups of cells or vesicles.[28,29] Values of zeta potential of various cationic lipid suspensions are shown in Table 1. Lipid **3** gave the highest zeta potential and lipid **1** gave the lowest value.

X-ray diffraction experiments of self-supporting cast films of the aqueous suspensions of **1**−**5** showed a series of higher order reflections characteristic of lamellar phases in their diffraction pattern. The unit lamellar widths of individual lipid aggregates are presented in Table 1. Incorporation of oxyethylene units at the linkage region increased the bilayer thickness of the lipid aggregates. The long spacing in the aggregates formed by lipids **1** and **2** were 54.5 and 59.2 Å, respectively, whereas their diether analogue, **5**, showed a long spacing of 48.7 Å. The increase in bilayer width due to oxyethylene linkages was lower for the unsymmetrical lipids **3** and **4**.

In general, the sizes of the aggregates formed by lipids **1**, **2**, and **3** were smaller in comparison with that of **4** and the control lipid, **5**. The hydrodynamic diameter of the aggregates formed by lipid **3** was the lowest, and interestingly, such lipid aggregates were found to have the highest zeta potential among the lipid suspensions studied. In the case of the other lipid formulations **1**, **2**, and **4**, the zeta potentials of the aggregates were substantially lower than that of the suspension of the control lipid, **5**. Notably, lipid **3** formed aggregates of the lowest hydrodynamic diameter and highest zeta potential when dispersed in water.

3.2. Thermal Properties. *3.2.1. Fluorescence Anisotropy.* To understand the relative order−disorder in the membranes

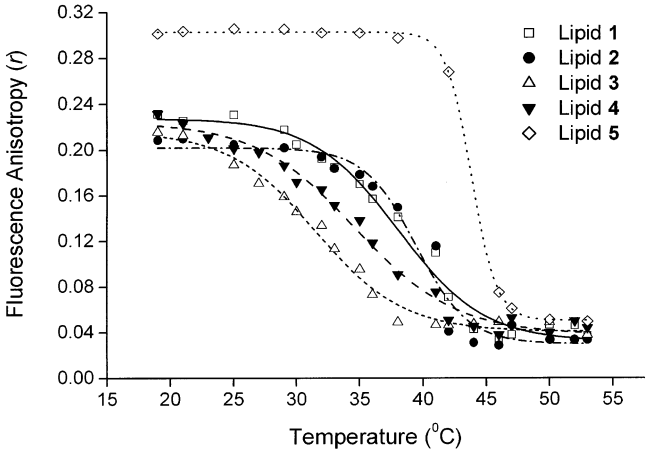

Figure 3. Changes in fluorescence anisotropy as a function of temperature due to DPH doped in various cationic lipid suspensions.

TABLE 2: Thermal Phase Transition Parameters as Obtained from the Steady State Anisotropy Experiment Due to DPH Doped in Various Lipid Aggregates

		anisotropy (r)		
lipid	T_m (°C)	$r_{25°C}$	$r_{30°C}$	r_{T_m}
1	38	0.23	0.21	0.13
2	39.2	0.21	0.20	0.13
3	31.7	0.19	0.15	0.12
4	34.6	0.20	0.18	0.13
5	43.8	0.31	0.30	0.18

formed by these new cationic lipids, the temperature induced hydrocarbon chain disorders were measured by determining the fluorescence anisotropy (r) of DPH as a function of temperature (Figure 3). The data summarizing the anisotropy sensed by DPH in various lipid aggregates are presented in Table 2.

The r vs T profiles in Figure 3 show systemic breaks related to the main-chain thermotropic phase transition processes for individual lipid assemblies. Comparison with the control lipid, **5**, revealed that the incorporation of oxyethylene units at the linkage region significantly decreased the gel to liquid crystalline phase transition temperature of the assemblies reported by DPH. Expectedly, the effects were more pronounced for the lipids with unsymmetrical linkages, i.e., **3** and **4**. Lipid **3**, which has an oxyethylene linkage only at the C-1 chain, showed the lowest gel to liquid crystalline phase transition temperature. Apart from lipid **5**, all the other lipid suspensions showed breaks in their r vs T plots, i.e., phase transition temperatures, ~3−7 °C lower than the T_m values observed under DSC studies (see below).

The anisotropy values of DPH for the lipid aggregates of **1**−**4** even in their solid gellike states were also found to be substantially lower than that for lipid **5**, suggesting a more disordered environment around the probe for DPH in these assemblies. Particulary low anisotropy values were observed for the unsymmetrical lipids **3** and **4** (Table 2). These trends were preserved throughout the temperature range in the gel state and were more obvious at elevated temperatures. This indicates a less ordered environment in the aggregates formed by lipids **3** and **4** at any temperatures below and above the phase transition. This could be explained from their unsymmetrical molecular structures. Due to mismatch at the linkage region, lipid packing in the aggregates of **3** and **4** could be relatively "loose" compared to their symmetrical counterparts **1** and **2**. For lipid **3**, the anisotropy value was very low, so that even at 25 °C itself, it was comparable to the r value of the control lipid, **5**, at its phase transition temperature.

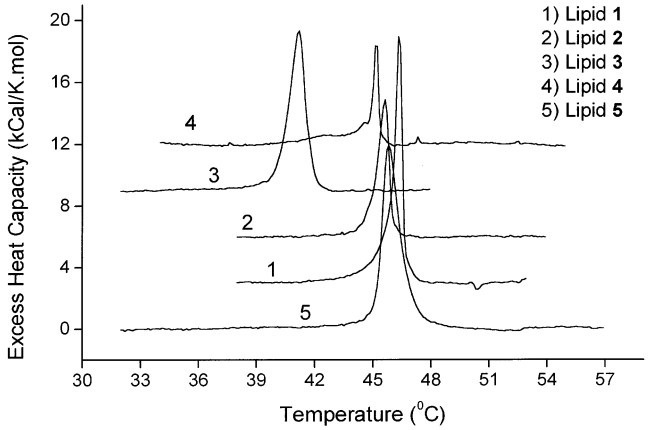

Figure 4. Thermotropic transitions as evidenced by the DSC on upscans. Thermograms of lipids **1**−**4** have been successively raised from the baseline by 3 kcal/(K·mol) steps for clarity.

TABLE 3: Thermotropic Parameters as Obtained from DSC Studies

	T_m[a] (°C)		ΔH[b] (kcal·mol^{-1})		CU[c]	
lipid	upscan	downscan	upscan	downscan	upscan	downscan
1	46.3	41.1	11.3	15.8	115	45
2	45.6	30.1	9.7	12.5	92	31
3	41.2	36.4	12.3	17.3	61	47
4	45.1	39.4	6.7	12.1	d	30
5	45.8	45.0	16.7	17.1	42	30

[a] The maximum deviation was ±0.1 °C. [b] Values varied within ±1 kcal·mol^{-1}. [c] Size of the cooperativity unit. [d] Could not be measured reliably due to baseline drifts.

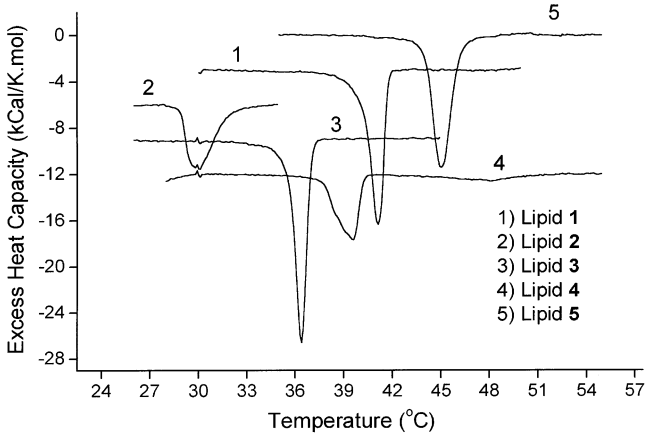

Figure 5. Thermotropic transitions as evidenced by the DSC on downscans. Thermograms of lipids **1**−**4** have been successively lowered from the baseline by 3 kcal/(K·mol) steps for clarity.

3.2.2. Differential Scanning Calorimetry. With all the lipid suspensions examined, the transitions were found to be fully reversible in differential scanning calorimetry. Well-behaved gel to liquid crystalline phase transitions were obtained for all the cationic lipid aggregates (Figure 4). The thermotropic properties as obtained from DSC for all the lipid aggregates are summarized in Table 3. A temperature lag was observed in thermograms of the cooling scans (liquid crystalline to gel phase transition) of the suspensions of all the lipids (Figure 5). Such a hysteresis was minimal for the control lipid, **5** (0.8 °C), and was maximum for the symmetrical lipid **2** (15.5 °C). Other lipids showed hysteresis of ~5 °C. Such high temperature lags are characteristics of a strongly first-order lipid phase transition.[30]

Several points may be noted from Table 3. First, these hydrated MLVs did not show considerable differences among

each other in phase transition temperatures as manifested in their DSC upscan thermograms. All the lipid aggregates in their heating scans showed phase transitions at temperatures between 45 and 46 °C, except for lipid, **3**, which gave a significantly lower T_m value (41 °C). Since these cationic lipids **1**−**5** only differ at the linkage region and have identical hydrocarbon chain length and headgroup molecular structure, the oxyethylene units do not significantly influence the T_m values in their heating scans. However, lipid **3** showed ∼5 °C lower gel to liquid crystalline phase transition temperature than the other lipids. This was also the case when transition temperatures were evaluated from the anisotropy values. Although the transition temperatures of the lipid suspensions followed a similar trend as that obtained from anisotropy vs temperature plots (Figure 3), the absolute values of transition temperatures obtained during DSC experiments were considerably different from those obtained by DPH anisotropy measurements. This can be explained by considering the fact that DPH, being a cylindrical hydrocarbon molecule, may align itself with the hydrocarbon chains perpendicular to the bilayer plane. In such a situation, this may reflect the order−disorder causative movements occurring at the deeper interior of the hydrophobic regions of a membranous assembly, and may not report the effects at the interfacial regions.

All these lipid formulations consistently showed single transition thermograms in both their heating and cooling scans. Lipid **2** sometimes showed multiple peaks at the same temperature region reported here. These transitions, however, resolved to individual peaks at lower scan rates. An unusual temperature lag of ∼15.5 °C was observed during the cooling scan of this lipid. However, the thermogram was totally reversible, subsequent upscan having the same transition temperature as the previous ones. This suggests that a highly stabilized "liquid crystalline" fluid phase might exist in the lipid aggregates of **2**. It is possible that, upon melting, lipid aggregates of **2** become highly hydrated. Cooling of the melted lipid aggregate at its full hydration may not immediately allow the "release" of the water molecules from these aggregates prior to its solidification to gel state. Other lipids except **5** also exhibited a similar temperature lag up to 5 °C. It is therefore reasonable to infer that the presence of oxyethylene units in **1**−**4** might help retention of water molecules in their melted state. Such hydrated melts resist loss of water molecules prior to their solidification to gel state during cooling.

In general, the enthalpy of transition of the heating scan was lower for lipids **1**−**4** in comparison with their diether analogue, **5**. Interestingly, all these lipids showed higher enthalpic contribution during their cooling scan (fluid to solid phase transition). In contrast, lipid **5** exhibited similar enthalpic contributions in both its heating and cooling scans.

The size of the cooperativity unit was also found to increase with the incorporation of oxyethylene linkages (Table 3). In all the aggregates, the liquid crystalline to gel phase transition was found to be less cooperative than the gel to liquid crystalline phase transition.

4. Discussion

In this paper we have presented the membrane-forming properties of four cationic lipids having a varying number of oxyethylene units between the pseudo-glyceryl backbone and the hydrophobic chains. **1** and **2** bear oxyethylene units at both hydrophobic chains yielding symmetrical lipids. In contrast, **3** and **4** have oxyethylene units only in one of the hydrocarbon chains. The properties of these new lipids were compared with a previously known cationic lipid **5** of the same hydrocarbon chain length bearing only single ether groups at the C-1 and C-2 positions of the linkage region.

The aggregation properties of these lipids in water were carefully investigated. Preparation of stable suspension of lipids in aqueous media was found to be particularly facile when lipids **1**−**4** were dispersed in water. For instance, while generation of a stable aqueous suspension of lipid **5** required repeated freeze−thaw cycles and an additional 10 min of sonication above phase transition temperatures, mild mechanical agitation of the lipid films of **1**−**4** produced optically stable aqueous suspensions. The presence of oxyethylene units at the linkage region presumably increases the hydration of lipids **1**−**4** in the aggregates. The resulting aqueous suspensions formed by lipids **1**−**4** were optically clear, whereas that of **5** yielded translucent suspensions.

TEM examination of the aqueous suspensions of lipids **1**, **2**, **4**, and **5** revealed the presence of spherical aggregates. In contrast, the lipid suspensions of **3** exhibited the presence of irregular morphologies. DLS measurements indicated that lipid **3** formed relatively smaller aggregates in water. Two distinct populations of aggregates were seen in the beginning of DLS measurements which gradually coalesced into a broad unimodal size distribution for the aggregate. Lipids **1**, **2**, and **4** showed narrow unimodal size distributions, whereas lipid **5** gave broad unimodal size distribution of its aggregates.

The zeta potential measurements indicated that the effective surface charge densities of the aqueous suspensions of lipids **1**, **2**, and **4** were substantially lower than that of lipid **5**. However, the aggregates formed from lipid **3** showed higher zeta potential than that of lipid **5**. The increase in hydration caused by these oxyethylene linkages should in turn lead to a better solvation of the charge. Such a deshielding of the surface charge may result in lower zeta potentials, which is observed in lipid aggregates of **1**, **2**, and **4**. The high zeta potential exhibited by lipid **3** may be due to the conformational arrangement of the chain having an oxyethylene group in the aggregates. In general, a lipid chain at the C-1 position of the pseudo-glyceryl backbone is known to penetrate deeper into the membrane.[31] If such conformational arrangements also exist in the present set of lipids, then the effect of oxyethylene unit of lipid **3** to increase the interfacial hydration should be lower than that of other lipids. Indirect evidence of such a conformational arrangement for this is evident from the results of the X-ray diffraction and DPH anisotropy studies.

X-ray diffraction investigations revealed that incorporation of oxyethylene units at the linkage region of a lipid increases the bilayer width of the membranous aggregates. This increase was conspicuous for the symmetrical lipids **1** and **2** in comparison with the unsymmetrical ones **3** and **4**. In the case of symmetrical lipids (**1** and **2**), introduction of each oxyethylene units increased the bilayer width by ∼5 Å. This is suggestive of an alignment of the oxyethylene units along the bilayer normal in the membranes formed by lipids **1** and **2**. The enhancement in bilayer thickness due to the oxyethylene linkages was comparatively lower for the unsymmetrical lipids. Introduction of two $-CH_2-CH_2-O-$ units at either the C-1 or C-2 position increased the bilayer width only by 3−5 Å. Interestingly, the membranes formed by lipid **3** in which a dioxyethylene unit is at the C-1 position of the pseudo-glyceryl backbone exhibited higher lamellar widths in comparison with **4**, which has the same unit at the C-2 position.

For the lipid aggregates **1**−**4** the anisotropy values of DPH were substantially lower than that of lipid **5**. Thus the incorpora-

tion of oxyethylene units at the linkages introduced disorder in the aggregates even in their solidlike gel states. The lowest anisotropy value was exhibited by lipid **3**. Its anisotropy value at the gel state was even comparable to the anisotropy values exhibited by **5** near its phase transition temperature. Being unsymmetrical, lipids **3** and **4** are expected to create more disorder in lipid packing in their aggregates compared to their symmetrical counterparts **1** and **2**. In glycerophospholipids, the fatty acid chain at the C-1 position protrudes deeper into the bilayer midplane.[31,32] If the same is true here, in the aggregates of lipid **3**, the chain bearing oxyethylene functionality should penetrate deeper into the membranous interior. Hence, the perturbation caused by the hydrophilic oxyethylene units in the hydrophobic environment of lipid chains may be expected to be more severe in the case of lipid **3** than that of lipid **4** if such a conformation is retained in these aggregates. Since the DPH anisotropy value reflects the disorder of this region, lipid **3** should exhibit the lowest anisotropy value, which is indeed the case.

All these lipid aggregates exhibited clear gel to liquid crystalline phase transitions as revealed by differential scanning calorimetry (DSC). The phase transitions were completely reversible. The phase transition temperatures (T_m) of lipids **1**, **2**, and **4** were comparable to that of lipid **5**. In contrast, the T_m of **3** was lower. More importantly, on cooling, all the lipids having oxyethylene groups exhibited a higher temperature lag (hysteresis) than that of lipid **5**, indicating first-order phase transitions in these assemblies. For lipid **5**, the heating and cooling scan showed comparable phase transition temperatures. However, the changes in T_m between heating and cooling scans were ~5 °C for lipids **1**, **3**, and **4** whereas it was as high as 15 °C for lipid **2**. This suggests that highly stabilized (hydrated) melted aggregates are present in these lipids. Upon melting, the hydration of the lipid aggregates will be higher and this highly hydrated fluid state for the oxyethylene lipids **1**−**4** should be more stabilized than that of the diether lipid, **5**. In general, the calorimetric enthalpies (ΔH_c) of the gel to liquid crystalline phase transition of oxyethylene lipid aggregates **1**−**4** were found to be lower than that of lipid **5**. Moreover, these aggregates showed a higher enthalpic contribution during their fluid to solid transition in contrast to the diether lipid **5**, which exhibited comparable enthalpies during its up- and downscans. The gel to liquid crystalline phase transitions of oxyethylene lipids **1**−**4** were more cooperative than their diether analogue, **5**. All the lipids showed lower cooperativities during their liquid crystalline to gel phase transition.

Having performed the physical characterizations of the membranes formed from the cationic oxyethylene lipids, it may be of interest to draw a possible correlation between the physical properties of these lipid aggregates and their biological activity. The lipids bearing oxyethylene links (**1**−**4**), when used in combination with the helper lipid dioleoylphosphatidylethanolamine (DOPE), are more efficient gene delivery agents compared to their simple diether lipid counterpart **5**.[17] Although the DNA delivery to a eukaryotic cell involves several steps, and the mechanism of such transfer is far from understood at the molecular level, the present studies provide useful insights as to why cationic oxyethylene lipids display superior gene transfer activity. It is evident from the present study that the incorporation of oxyethylene units at the linkage region of a cationic lipid significantly alters the aggregate properties in comparison with that of the conventional lipid **5**. Notably, the oxyethylene units bring about significant disorder in the hydrocarbon chain packing in these lipid aggregates. This explains the increased transfection activities of these lipids, because it has been previously shown that the membrane perturbation due to the vector lipids is an important factor in cationic liposome mediated DNA delivery.[33] Insertion of oxyethylene units in the linkage region also influences hydration of the resulting aggregates. Hydration of lipoplexes is known to influence gene transfer events.[34] Even among the oxyethylene lipids **1**−**4** there were subtle but important differences. The transfection efficiencies of the unsymmetrical lipids **3** and **4** were found to be higher than their symmetrical counterparts **1** and **2**. Again the mismatch in the linkage region helped disturb the lipid packing in such aggregates, making them susceptible to complex with DNA. In particular, the unsymmetrical lipid **3** has shown exceptional transfection capabilities in the presence of serum. The physical-chemical studies also show that the aggregates formed by lipid **3** are unique among this class of molecules. Lipid **3** membranes manifested the lowest hydrodynamic diameter and highest zeta potentials. These parameters are favorable for DNA complexation.[35] This is quite important in the context that the condensation of DNA by cationic liposomes is believed to be one of the major events in the transfection process.[36,37] Further, these aggregates were of irregular morphologies and possessed maximally disordered hydrocarbon chain environments. Notably, the gel to liquid crystalline phase transition temperature of this lipid aggregate was the lowest in this series of lipids and was comparable to the physiological temperature. Thus, it is not a mere coincidence that lipid **3** in the presence of DOPE was the most efficient transfection reagent among these oxyethylene lipids. Therefore, the present study clearly demonstrates that the aggregation behavior and the surface properties of these cationic lipid membranes may have significant relevance to their biological activity.

Acknowledgment. This work was supported by the Swarnajayanti Fellowship grant of the Department of Science & Technology awarded to S.B. We thank CSIR, New Delhi, for the award of a Senior Research Fellowship to P.V.D.

References and Notes

(1) Miller, A. D. *Angew. Chem., Int. Ed.* **1998**, *37*, 1768−1785.
(2) Behr, J. P. *Acc. Chem. Res.* **1993**, *26*, 274−278.
(3) Felgner, P. L.; Gadek, T. R.; Holm, M.; Roman, R.; Chan, H. W.; Wenz, M.; Northrop, J. P.; Ringold, G. M.; Danielsen, M. *Proc. Nat. Acad. Sci. U.S.A.* **1987**, *84*, 7413−7417.
(4) Felgner, J. H.; Rajkumar,; Sridhar, C. N.; Wheeler, C. J.; Tsai, Y. J.; Border, R.; Ramsey, P.; Martin, M.; Felgner, P. L. *J. Biol. Chem.* **1994**, *269*, 2550−2561.
(5) Felgner, P. L.; Ringold, G. M. *Nature* **1989**, *337*, 387−388.
(6) Elizabeth, G. N.; Gordon, D.; Yang, Z.; Xu, L.; San, H.; Gregory, E. P.; Wu, B.; Gao, X.; Huang, L.; Gary, J. N. *Hum. Gene Ther.* **1992**, *3*, 649−656.
(7) Caplen, N. J.; Alton, E. W.; Middleton, P. G.; Dorin, J. R.; Stevenson, B. J.; Gao, X.; Durham, S. R.; Jeffery, P. K.; Hodson, M. E.; Coutelle, C.; Huang, L.; Porteous, D. J.; Williamson, R.; Geddes, D. M. *Nat. Med.* **1995**, *1*, 39−46.
(8) Epand, R. M.; Kraayenhof, R. *Chem. Phys. Lipids* **1999**, *101*, 57−64.
(9) Bhattacharya, S.; Haldar, S. *Langmuir* **1995**, *11*, 4748−4757.
(10) Bhattacharya, S.; Haldar, S. Unpublished results.
(11) Song, Y. K.; Liu, F.; Chu, S.; Liu, D. *Hum. Gene Ther.* **1997**, *8*, 1585−1592.
(12) Ghosh, Y. K.; Visweswariah, S. S.; Bhattacharya, S. *FEBS Lett.* **2000**, *473*, 341−344.
(13) Ghosh, Y. K.; Visweswariah, S. S.; Bhattacharya, S. *Bioconjugate Chem.* **2002**, *13*, 378−384.
(14) Bhattacharya, S.; Dileep, P. V. *Tetrahedron Lett.* **1999**, *40*, 8167−8170.

(15) Woodle, M. C.; Lasic, D. *Biochem. Biophys. Acta* **1992**, *1113*, 171−199.
(16) Schule, U.; Schmidt, H.-W.; Safinya, C. *Bioconjugate Chem.* **1999**, *10*, 548−552.
(17) Dileep, P. V.; Antony, A.; Bhattacharya, S. *FEBS Lett.* **2001**, *509*, 327−331.
(18) Zelphati, O.; Uyechi, L. S.; Barron, L. G.; Szoka, F. C., Jr. *Biochim. Biophys. Acta* **1998**, *1390*, 119−133.
(19) Kimizuka, N.; Kawasaki, T.; Kunitake, T. *J. Am. Chem. Soc.* **1993**, *115*, 4387−4388.
(20) Kimizuka, N.; Kawasaki, T.; Hirata, K.; Kunitake, T. *J. Am. Chem. Soc.* **1998**, *120*, 4094−4104.
(21) Chen, R. F.; Bowman, R. L. *Science* **1965**, *147*, 729−732.
(22) Lakowicz, J. *Principles of Fluorescence Spectroscopy*, 1st ed.; Plenum Press: New York and London, 1983.
(23) Shinitzky, M.; Barenholtz, Y. *Biochim. Biophys. Acta* **1978**, *525*, 367−394.
(24) Shinitzky, M.; Inbar, M. *Biochim. Biophys. Acta* **1976**, *433*, 133−149.
(25) Hinz, H.; Sturtevant, J. M. *J. Biol. Chem.* **1972**, *247*, 6071−6075.
(26) Sturtevant, J. M. *Proc. Natl. Acad. Sci. U.S.A.* **1982**, *79*, 3963−3967.
(27) Kraayenhof, R.; Sterk, G. J.; Wong Fong Sang, H. W. *Biochemistry* **1993**, *32*, 10057−10066.
(28) Cevc, G. *Chem. Phys. Lipids* **1993**, *64*, 163−186.
(29) Petty, H. R.; Ware, B. R.; Wasserman, S. I. *Biophys. J.* **1980**, *30*, 41−50.
(30) Marsh, D. *Chem. Phys. Lipids* **1991**, *57*, 109−120.
(31) Pearson, R. H.; Pascher, I. *Nature* **1979**, *281*, 499−501.
(32) Seelig, J.; Brown, J. L. *FEBS Lett.* **1978**, *92*, 41−44.
(33) Mui, B.; Ahkong, Q. F.; Chow, L.; Hope, M. *Biochim. Biophys. Acta* **2000**, *1467*, 281−292.
(34) Hirsch-Lerner, D.; Barenholz, Y. *Biochim. Biophys. Acta* **1999**, *1461*, 47−57.
(35) Son, K. K.; Tkach, D.; Patel, D. H. *Biochim. Biophys. Acta* **2000**, *1468*, 11−14.
(36) Zabner, J.; Fasbender, A. J.; Moninger, T.; Poellinger, K. A.; Walsh, M. J. *J. Biol. Chem.* **1995**, *270*, 18997−19007.
(37) Gershon, H.; Ghirlando, R.; Guttman, S. B.; Minsky, A. *Biochemistry* **1993**, *32*, 7143−7151.